Journal of Alloys and Compounds 509 (2011) 2659–2662

Contents lists available at ScienceDirect

Journal of Alloys and Compounds

journal homepage: www.elsevier.com/locate/jallcom

Luminescence properties of $SrIn_2O_4:Eu^{3+}$ incorporated with Gd^{3+} or Sm^{3+} ions

Hailong Wang, Lianhua Tian*

Department of Physics, Yanbian University, Yanji 133002, China

ARTICLE INFO

Article history:
Received 10 June 2010
Received in revised form
17 November 2010
Accepted 1 December 2010
Available online 7 December 2010

Keywords:
Potoluminescence
$SrIn_2O_4:Eu^{3+},Gd^{3+}$
$SrIn_2O_4:Eu^{3+},Sm^{3+}$

PACS:
78.55.−m

ABSTRACT

The photoluminescence (PL) properties of $SrIn_2O_4:Eu^{3+},Gd^{3+}$ and $SrIn_2O_4:Eu^{3+},Sm^{3+}$ are investigated in this work. When the Gd^{3+} ions are introduced in this compound, the average distance metal-oxygen is increased, and then the vibration of lattice is decreased. It results in that the nonradiation of Eu^{3+} is decreased. Therefore, the emissions of $SrIn_2O_4:Eu^{3+}$ are increased. However, little of energy transfer occurs from Gd^{3+} to Eu^{3+} ions. When the Sm^{3+} ions are introduced into $SrIn_2O_4:Eu^{3+}$, the energy transfers occur from the CTS of O^{2-}–Sm^{3+} to Sm^{3+} and Eu^{3+} ions, from the host absorption to Eu^{3+} ions, and from Sm^{3+} to Eu^{3+} ions, but not from the host absorption to Sm^{3+} ions.

1. Introduction

The development of displays or lamps has always been accompanied by improvements in the phosphors used. Great effort has been made to discover host materials as well as activators with high performance for phosphor applications. In the last several years, the luminescent properties of the rare earth doped borates, aluminates and gallates have been extensively studied [1–4]. Indium belongs to the same IIIA group of periodic table of elements with boron, aluminum and gallium and exhibits similar chemical properties. Among the indium-based oxides, $SrIn_2O_4$ and $CaIn_2O_4$ are found to be an attractive host lattice for rare earth ions which is evident from the recent reports by different research groups. The semiconductor $SrIn_2O_4$ serves as host lattice for Pr^{3+}, Tb^{3+} and Eu^{3+} activators for red and green phosphors, respectively [5–10].

On the other hand, the electronic energy transfer or relaxation plays an important role in the inorganic phosphors. It is important to understand the kinetic properties of trivalent rare earth ions such as Gd^{3+}, Sm^{3+}, and Eu^{3+} for the development of the visible luminescent materials excited with UV or VUV light. The energy transfer in some host materials from Gd^{3+} or Sm^{3+} ions to Eu^{3+} dopant is well known [4,11–18]. In this work, the photoluminescence properties of $SrIn_2O_4:Eu^{3+}$ codoping Gd^{3+} or Sm^{3+}ions are investigated. With introduced Gd^{3+} ions in $SrIn_2O_4:Eu^{3+}$, the emission intensity of $SrIn_2O_4:Eu^{3+}$ is increased. However, in $SrIn_2O_4$, the energy transfer does not occur from ^6P levels of Gd^{3+} to Eu^{3+}. With the Sm^{3+} incorporation, the energy transfers occur from the CTS of O^{2-}–Sm^{3+} to Sm^{3+} and Eu^{3+} ions, from the host absorption to Eu^{3+} ions, and from Sm^{3+} to Eu^{3+} ions, but not from the host absorption to Sm^{3+} ions.

2. Experimental

The phosphors $SrIn_2O_4:Eu^{3+},Sm^{3+}$ and $SrIn_2O_4:Eu^{3+},Gd^{3+}$ were prepared by the solid state reaction method at high temperature. The stoichiometric staring materials $SrCO_3$ (Analytical reagent), In_2O_3 (99.99%), Eu_2O_3 (99.99%), Sm_2O_3 (99.99%), and Gd_2O_3 (99.9%) were ground in an agate mortar and heated at 1300 °C for 4 h.

The excitation and emission spectra were recorded on a Hitachi F-4500 with a 700 W Xe lamp. The structures of these powders were recorded by X-ray powder diffraction (XRD) using Cu Kα ($\lambda = 0.15178$ nm) radiation on a TD-2500 X-ray diffractometer.

3. Results and discussion

3.1. $SrIn_2O_4:Eu^{3+},Gd^{3+}$

The XRD patterns of $SrIn_{1.995-x}O_4:Eu^{3+}(0.5\%),Gd^{3+}(x = 0\%, 30\%,$ and 50%) are shown in Fig. 1. The structure of $SrIn_2O_4$ is isostructural to $CaFe_2O_4$ and belongs to the orthorhombic system. In this structure the In element is located at two 4c positions corresponding to a Cs point site symmetry. For both sites, In(1) and In(2) have six coordination environment with small variations in the In–O bond lengths. Among them, the site In(2) is more regular; its point symmetry is relatively close to C_{2v}. The In(1)O6 octahedron shares its edges with another In(1)O6 octahedron forming a repeat unit and these units share corners with a similar unit formed by

* Corresponding author. Tel.: +86 433 2732221.
E-mail address: lhtian@ybu.edu.cn (L. Tian).

0925-8388/$ – see front matter © 2010 Published by Elsevier B.V.
doi:10.1016/j.jallcom.2010.12.001

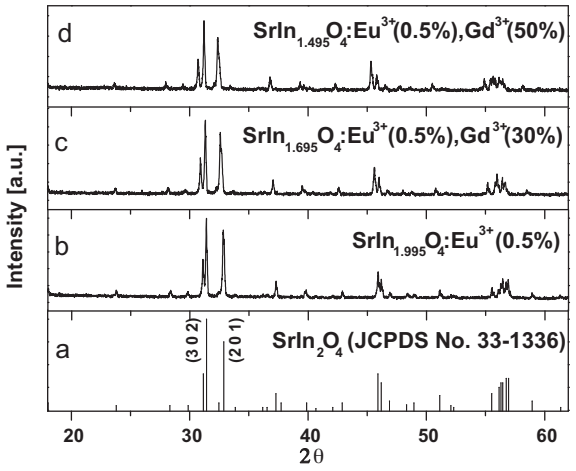

Fig. 1. XRD patterns for (a) $SrIn_2O_4$ (JCPDS No. 33-1336), (b) $SrIn_{1.995}O_4$:Eu^{3+}(0.5%), (c) $SrIn_{1.695}O_4$:Eu^{3+}(0.5%),Gd^{3+}(30%), and (d) $SrIn_{1.495}O_4$:Eu^{3+}(0.5%),Gd^{3+}(50%).

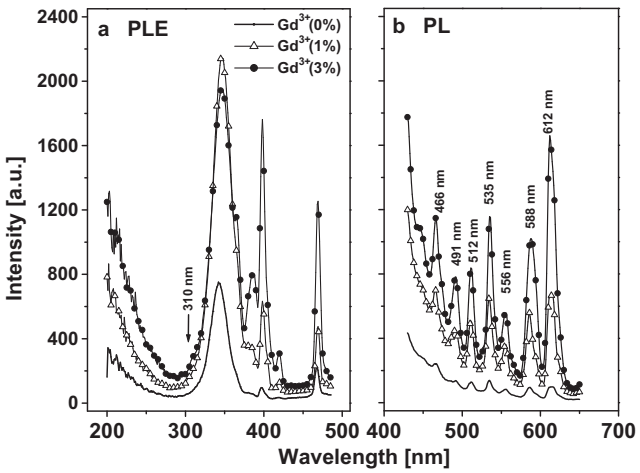

Fig. 2. (a) Excitation spectra (PLE) (λ_{em} = 612 nm) of $SrIn_{1.995}O_4$:Eu^{3+}(0.5%) (–), $SrIn_{1.985}O_4$:Eu^{3+}(0.5%),Gd^{3+}(1%) (△), and $SrIn_{1.965}O_4$:Eu^{3+}(0.5%),Gd^{3+}(3%) (●). (b) Photoluminescence spectra (PL) (λ_{ex} = 397 nm) of $SrIn_{1.995}O_4$:Eu^{3+}(0.5%) (–), $SrIn_{1.985}O_4$:Eu^{3+}(0.5%),Gd^{3+}(1%) (△), and $SrIn_{1.965}O_4$:Eu^{3+}(0.5%),Gd^{3+}(3%) (●).

In(2)O6 octahedra resulting in a zig-zag chain structure [19,20]. The XRD pattern of $SrIn_2O_4$:Eu^{3+}(0.5%) is very much consistent with the JCPDS 33-1336. Considering the size of the ions (ionic radii of Gd^{3+}, Eu^{3+}, and In^{3+} with C.N. = 6 are 0.938, 0.947, and 0.800 Å, respectively) and the lattice sites, the Gd^{3+} ion can be substituted into the In^{3+} site, leading to $SrIn_{2-x}Gd_xO_4$:Eu^{3+}. The XRD patterns of $SrIn_{1.995-x}O_4$:Eu^{3+}(0.5%),Gd^{3+}(x = 0%, 30%, and 50%) are observed to be very similar to that of $SrIn_2O_4$. However, the powder XRD patterns show a shift towards lower angles with increasing Gd^{3+} concentration as shown in Fig. 1. The calculated lattice parameters of $SrIn_{1.995-x}O_4$:Eu(0.5%),Gd(x) are listed in Table 1. The lattice parameters show an increase in all three parameters with increasing concentration of Gd^{3+} as expected based on the bigger size of Gd^{3+} ion than that of In^{3+} ion. It confirms that a complete solid solution in $SrIn_{2-x}Gd_xO_4$ is obtained. Because the both end of members, $SrIn_2O_4$ and $SrGd_2O_4$, are isostructural compounds.

The excitation and photoluminescence spectra of $SrIn_{1.995-x}O_4$:Eu^{3+}(0.5%),Gd^{3+}(x = 0%, 1% and 3%) are shown in Fig. 2. The excitation spectra exhibit a broad absorption bands centered at 342 nm. Three sharp absorption peaks at 385, 397 and 468 nm are also observed, which are due to the excitation of Eu^{3+} from the ground $^7F_0$ state to various higher excited states. The broad band at 342 nm in the excitation spectrum is attributed to the host lattice absorption since the host $SrIn_2O_4$ is a semiconductor with band gap energy of 3.6 eV [5,21].

It can be seen that doping Gd^{3+} ions into $SrIn_2O_4$:Eu^{3+} changes the intensity of excitation bands in Fig. 2(a). With the increasing of the Gd^{3+} concentration, intensity of absorption band around 342 nm increases and reaches a maximum at Gd^{3+} concentration of 1%. Especially, it is enhanced obviously for the sharp excitation peaks in the range of 350–470 nm originated the *f*–*f* transitions of Eu^{3+} ions. The excitation peak at 397 nm of $SrIn_{1.965}O_4$:Eu^{3+}(0.5%),Gd^{3+}(3%) is enhanced about 10 times than that of Gd^{3+} free $SrIn_2O_4$:Eu^{3+}. In the excitation spectrum of $SrIn_{1.965}O_4$:Eu^{3+}(0.5%),Gd^{3+}(3%), it also can be seen that there is a very weak excitation band at about 310 nm which is due to the $^8S_{7/2} \rightarrow {}^6P_J$ transition of Gd^{3+} ion. It is speculated that the effect of energy transfer from Gd^{3+} to Eu^{3+} is very weak. On the other hand, according to the excitation spectra of $SrIn_{1.995-x}O_4$:Eu^{3+}(0.5%),Gd^{3+}(x), the weak broad band below 296 nm corresponds to the charge transfer state (CTS) between Eu^{3+} and O^{2-} [9,10], which is increased with incorporation of Gd^{3+} ions.

The PL spectra of $SrIn_2O_4$:Eu^{3+},Gd^{3+} exhibit the emission lines from the $^5D_{0,1,2}$ excited states to the ^7F_J ground states of Eu^{3+}, i.e., $^5D_2 \rightarrow {}^7F_0$ (466 nm), $^5D_2 \rightarrow {}^7F_2$ (491 nm), $^5D_1 \rightarrow {}^7F_3$ (512 nm), $^5D_1 \rightarrow {}^7F_1$ (535 nm), $^5D_1 \rightarrow {}^7F_2$ (556 nm), $^5D_0 \rightarrow {}^7F_1$ (588 nm), and $^5D_0 \rightarrow {}^7F_2$ (612 nm) as shown in Fig. 2(b) [9]. The dependence of the luminescence efficiency on the content of Gd^{3+} ion under excitation at 397 nm is shown in Fig. 3. When Gd^{3+} ion is incorporated into $SrIn_2O_4$:Eu^{3+}, the luminescence intensity is increased up to a factor of ten times compared with that of Gd^{3+} free $SrIn_2O_4$:Eu^{3+}. With increasing the concentration of Gd^{3+}, the luminescence intensity of the nominal composition $SrIn_{1.995-x}O_4$:Eu^{3+}(0.5%),Gd^{3+}(x) is enhanced until x = 3%.

The incorporation of Gd^{3+} into $SrIn_2O_4$:Eu^{3+} increases the average distance metal-oxygen due to the radius of Gd^{3+} ion larger than that of In^{3+} ion. It results in that the nonradiation of Eu^{3+} is decreased due to the decrease of the vibration of lattice. Therefore,

Table 1
Calculated lattice parameters of $SrIn_{1.995-x}O_4$:Eu^{3+}(5%),Gd^{3+}/Sm^{3+}(x) (x = 0, 0.3 and 0.5).

x	a (Å)	b (Å)	c (Å)
0.0	9.8325	11.4886	3.2740
Gd (x = 0.3)	9.8327	11.5477	3.3003
Gd (x = 0.5)	9.8491	11.5889	3.3197
Sm (x = 0.3)	9.8560	11.5897	3.3112
Sm (x = 0.5)	9.8870	11.6546	3.3302

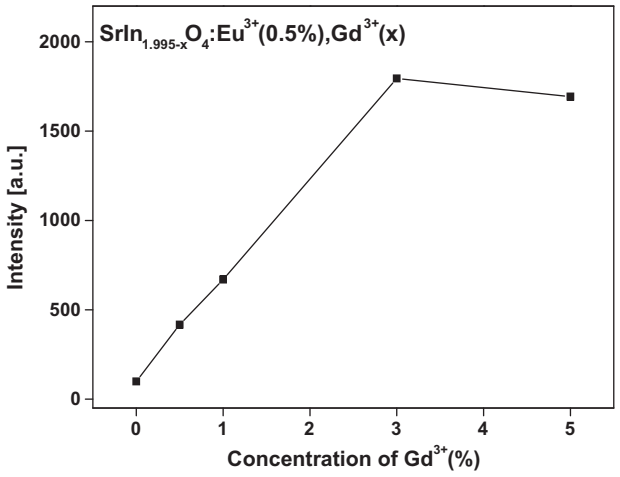

Fig. 3. Photoluminescence intensity at 612 nm as a function of Gd^{3+} concentration in $SrIn_{1.995}O_4$: Eu^{3+}(0.5%) excited with 397 nm.

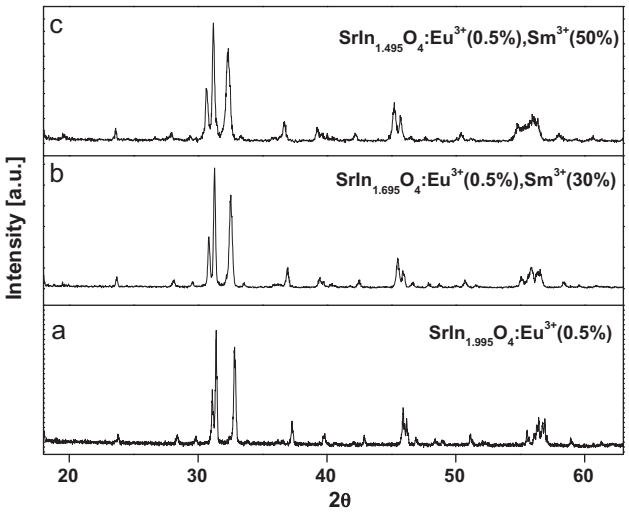

Fig. 4. XRD patterns for (a) $SrIn_{1.995}O_4:Eu^{3+}(0.5\%)$, (b) $SrIn_{1.695}O_4:Eu^{3+}(0.5\%)$, $Sm^{3+}(30\%)$, and (c) $SrIn_{1.495}O_4:Eu^{3+}(0.5\%),Sm^{3+}(50\%)$.

the emission intensity of $SrIn_2O_4:Eu^{3+}$ is enhanced by incorporation of Gd^{3+} ions. On the other hand, In^{3+} substituted with Gd^{3+} ions in $SrIn_2O_4$ decreases the symmetry of Eu^{3+} site in $SrIn_2O_4$ lattice. The structural change results from the ionic size of the constituents in this type structure, i.e. the substitution of In by the larger Gd^{3+} leads to the decrease of the centrosymmetric nature of the Eu^{3+} site in $SrIn_2O_4$. As discussed above, it is clearly shown in Fig. 2 that the emission of the electronic dipole $^5D_0 \rightarrow {}^7F_2$ transition at ca. 612 nm grows rapidly in comparison with that of the magnetic dipole $^5D_0 \rightarrow {}^7F_1$ transition at 588 nm as the Gd^{3+} incorporates in the lattice. It also confirms the decrease of the centrosymmetric nature of the Eu^{3+} site in $SrIn_2O_4$.

3.2. $SrIn_2O_4:Eu^{3+},Sm^{3+}$

The XRD pattern of $SrIn_{1.995-x}O_4:Eu^{3+}(0.5\%),Sm^{3+}(x)$ are shown in Fig. 4. The powder XRD patterns show a shift towards lower angles with the increasing of Sm^{3+} concentration in a similar way to Gd^{3+}. The calculated lattice parameters of $SrIn_{1.995-x}O_4:Eu(0.5\%),Sm(x)$ are listed in Table 1. The lattice parameters also shows an increase in all three parameters with increasing concentration of Sm^{3+} because of larger radius of Sm^{3+} ion than that of In^{3+} ion. It also confirms that a complete solid solution in $SrIn_{2-x}Sm_xO_4$ is obtained.

Shown in Fig. 5(a) are the excitation spectra of $SrIn_{1.995-x}O_4:Eu^{3+}(0.5\%),Sm^{3+}(x=0\%$ and $1\%)$. The excitation spectrum of $SrIn_{1.985}O_4:Eu^{3+}(0.5\%),Sm^{3+}(1\%)$ monitored at 618 nm consists of five peaks in the wavelength range from 300 to 450 nm in comparison with that of Sm^{3+} free $SrIn_2O_4:Eu^{3+}$. The broad excitation band is centered at 312 nm due to charge transfer absorption of O^{2-}–Sm^{3+}. The strong sharp absorption bands are observed at 366, 383, and 397 nm due to the *f–f* transitions of Eu^{3+} ion. In the region around 410 nm, main absorption of Sm^{3+} ion can be seen obviously, which is ascribed to the $^6H_{5/2} \rightarrow {}^4K_{11/2}$ transition [4,16,18]. It is well-known that Sm^{3+} ions exhibit absorption at about 410 nm in many host lattices [15–18].

The PL spectra of $SrIn_{1.995}O_4:Eu^{3+}(0.5\%)$, $SrIn_{1.985}O_4:Eu^{3+}(0.5\%),Sm^{3+}(1\%)$ and $SrIn_{1.990}O_4:Sm^{3+}(1\%)$ are shown in Fig. 5(b). For $SrIn_{1.995}O_4:Eu^{3+}(0.5\%)$, the PL spectrum excited at 342 nm exhibits the emission lines at $^5D_2 \rightarrow {}^7F_2$ (491 nm), $^5D_1 \rightarrow {}^7F_3$ (512 nm), $^5D_1 \rightarrow {}^7F_1$ (535 nm), $^5D_1 \rightarrow {}^7F_2$ (556 nm), $^5D_0 \rightarrow {}^7F_1$ (586 nm), and $^5D_0 \rightarrow {}^7F_2$ (615 nm). For Sm^{3+} ion, the closely lying lower $^4G_{5/2}$, $^4G_{7/2}$, and $^4F_{3/2}$ states were populated

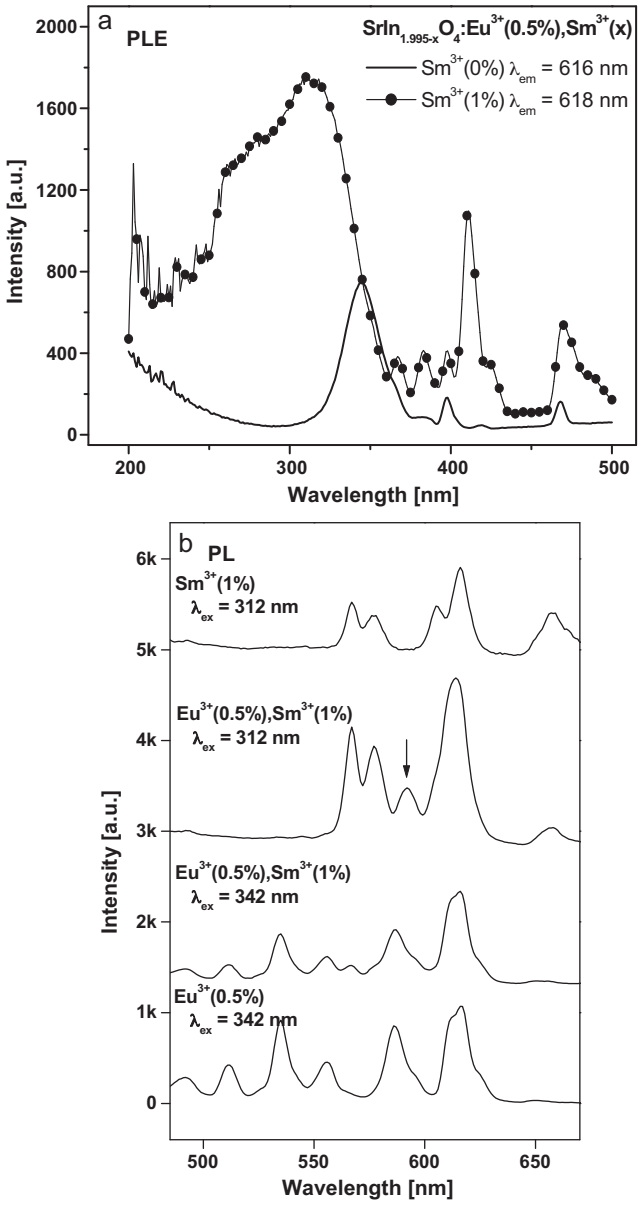

Fig. 5. (a) Excitation spectra (PLE) of $SrIn_{1.995}O_4:Eu^{3+}(0.5\%)$ ($\lambda_{em} = 615$ nm) (–) and $SrIn_{1.985}O_4:Eu^{3+}(0.5\%),Sm^{3+}(1\%)$ ($\lambda_{em} = 618$ nm) (●). (b) Photoluminescence spectra (PL) of $SrIn_{1.995}O_4:Eu^{3+}(0.5\%)$ ($\lambda_{ex} = 342$ nm), $SrIn_{1.985}O_4:Eu^{3+}(0.5\%),Sm^{3+}(1\%)$ ($\lambda_{ex} = 342$ nm), $SrIn_{1.985}O_4:Eu^{3+}(0.5\%),Sm^{3+}(1\%)$ ($\lambda_{ex} = 312$ nm) and $SrIn_{1.990}O_4:Sm^{3+}(1\%)$ ($\lambda_{ex} = 312$ nm).

and emission is obtained. The emissions of $SrIn_{1.990}O_4:Sm^{3+}(1\%)$ under excitation at 312 nm are observed at 567 nm, 578 nm, 605 nm and 616 nm and correspond to the $^4G_{5/2} \rightarrow {}^6H_{5/2}$, $^4G_{7/2} \rightarrow {}^6H_{9/2}$, $^4F_{3/2} \rightarrow {}^6H_{7/2}$ and $^4F_{3/2} \rightarrow {}^6H_{9/2}$ transitions of Sm^{3+} ion respectively. The main luminescence peaks in spectrum of $SrIn_{1.985}O_4:Eu^{3+}(0.5\%),Sm^{3+}(1\%)$ excited at 312 nm are observed at 567 and 577 nm due to the $^4G_{5/2} \rightarrow {}^6H_{5/2}$ and $^4G_{7/2} \rightarrow {}^6H_{9/2}$ transitions of Sm^{3+} ion respectively. The emission peak at 592 nm corresponds to the $^5D_0 \rightarrow {}^7F_1$ transition of Eu^{3+}. The peak at 615 nm corresponds to the overlap of the transitions of $^4F_{3/2} \rightarrow {}^6H_{9/2}$ of Sm^{3+} ion and $^5D_0 \rightarrow {}^7F_2$ of Eu^{3+} ion. However, when the spectrum of $SrIn_{1.985}O_4:Eu^{3+}(0.5\%),Sm^{3+}(1\%)$ is excited at 342 nm, it is similar with that of Sm^{3+} free $SrIn_{1.995}O_4:Eu^{3+}(0.5\%)$. It is confirmed further that the energy transfers occur from the CTS of O^{2-}–Sm^{3+} to Sm^{3+} and Eu^{3+} ions, or from the host absorption to Eu^{3+} ions, but not from the host absorption to Sm^{3+} ions. However, the part of

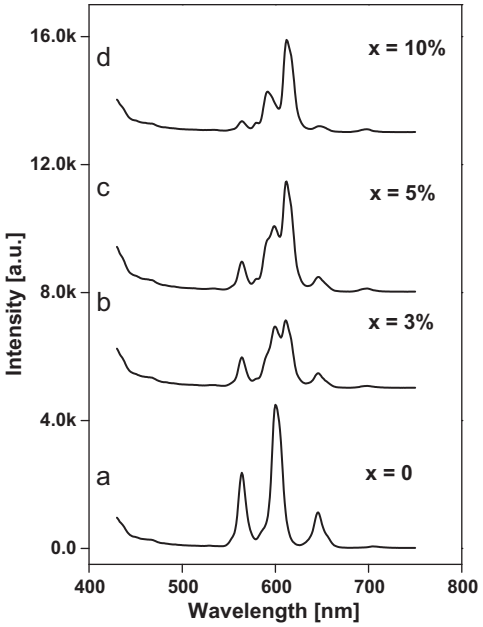

Fig. 6. The PL spectra of $SrIn_{1.990-x}O_4:Eu^{3+}(x),Sm^{3+}(1\%)$ with the Eu^{3+} concentration of: (a) $x = 0\%$; (b) $x = 3\%$; (c) $x = 5\%$; (d) $x = 10\%$; obtained exciting at the wavelength of 410 nm.

energy transfer from the CTS of O^{2-}–Sm^{3+} to Eu^{3+} is much smaller than that to Sm^{3+} ion.

On the other hand, Fig. 6 shows the PL spectra of $SrIn_{1.990-x}O_4:Eu^{3+}(x),Sm^{3+}(1\%)$ ($x = 0\%$, 3%, 5%, and 10%) excited at 410 nm which is corresponding to the $^6H_{5/2} \rightarrow {}^4K_{11/2}$ transition of Sm^{3+}. With increasing the concentration of Eu^{3+}, the intensity of the emission line at 615 nm which is ascribed to the $^5D_0 \rightarrow {}^7F_2$ transition of Eu^{3+} is increased compared to the line at 600 nm which is ascribed to the $^4G_{7/2} \rightarrow {}^6H_{7/2}$ transition of Sm^{3+}. It is confirmed that the energy transfer is occurred from Sm^{3+} to Eu^{3+} ions.

4. Conclusion

The PL properties of $SrIn_2O_4:Eu^{3+},Gd^{3+}$ and $SrIn_2O_4:Eu^{3+},Sm^{3+}$ are investigated in this work. The excitation spectrum of $SrIn_2O_4:Eu^{3+}$ shows a broad excitation band with a maximum at 342 nm, a weak peak at 397 nm and a weak broad band below 296 nm corresponds to the charge transfer state (CTS) between O^{2-} and Eu^{3+}. The PL spectrum excited at 397 nm shows mainly at 466, 491, 512, 535, 556, 588 and 612 nm. When the Gd^{3+} ions are introduced in this compound, the average distance metal-oxygen is increased, and then the vibration of lattice is decreased. It results in that the nonradiation of Eu^{3+} is decreased. Therefore, the emissions of Eu^{3+} are increased until $x = 3\%$. However, little of energy transfer occurs from Gd^{3+} to Eu^{3+} ion. When the Sm^{3+} ions are introduced into $SrIn_2O_4:Eu^{3+}$, The excitation spectrum of $SrIn_{1.985}O_4:Eu^{3+}(0.5\%),Sm^{3+}(1\%)$ monitored at 618 nm consists of five peaks in the wavelength range from 300 to 450 nm compared to Sm^{3+} free $SrIn_2O_4:Eu^{3+}$. The main luminescence peaks in spectrum of $SrIn_{1.985}O_4:Eu^{3+}(0.5\%),Sm^{3+}(1\%)$ are observed at 567 and 577 nm due to the $^4G_{5/2} \rightarrow {}^6H_{5/2}$ and $^4G_{7/2} \rightarrow {}^6H_{9/2}$ transitions of the Sm^{3+} ion respectively. The peak at 615 nm corresponds to the overlap of the transitions of $^4F_{3/2} \rightarrow {}^6H_{9/2}$ of Sm^{3+} ion and $^5D_0 \rightarrow {}^7F_2$ of Eu^{3+} ion. The emission peak at 592 nm corresponds to the $^5D_0 \rightarrow {}^7F_1$ transition of Eu^{3+}. However, when the spectrum of $SrIn_{1.985}O_4:Eu^{3+}(0.5\%),Sm^{3+}(1\%)$ is excited at 342 nm, it is similar with that of Sm^{3+} free $SrIn_{1.995}O_4:Eu^{3+}(0.5\%)$. In PL spectra of $SrIn_{1.990-x}O_4:Eu^{3+}(x),Sm^{3+}(1\%)$ excited at 410 nm, with increasing the concentration of Eu^{3+}, the intensity of the $^5D_0 \rightarrow {}^7F_2$ transition of Eu^{3+} is increased in comparison with the $^4G_{7/2} \rightarrow {}^6H_{7/2}$ transition of Sm^{3+}. It is confirmed that the energy transfers occur from the CTS of O^{2-}–Sm^{3+} to Sm^{3+} and Eu^{3+} ions, from the host absorption to Eu^{3+} ions, and from Sm^{3+} to Eu^{3+} ions, but not from the host absorption to Sm^{3+} ions.

References

[1] L. Tian, B.Y. Yu, C.H. Pyun, H.L. Park, S.-I. Mho, Solid State Commun. 129 (2004) 43.
[2] K.G. Lee, B.Y. Yu, C.H. Pyun, S.-I. Mho, Solid State Commun. 122 (2002) 485.
[3] J.S. Kim, H.I. Kang, G.C. Kim, T.W. Kim, Y.H. Hwang, H.K. Kim, S.I. Mho, S.D. Han, Solid State Commun. 126 (2003) 515.
[4] S.K. Sharma, S.S. Pitale, M.M. Malik, M.S. Qureshi, R.N. Dubey, J. Alloys Compd. 482 (2009) 468.
[5] F.S. Kao, T.M. Chen, J. Lumin. 156 (2001) 84.
[6] H. Yamamoto, M. Abe, M. Ogura, S. Mitsumine, K. Uheda, S. Okamoto, J. Electrochem. Soc. 154 (2007) J15.
[7] A. Baszczuk, M. Jasiorski, M. Nyk, J. Hanuza, M. Mączka, W. Stręk, J. Alloys Compd. 394 (2005) 88.
[8] N. Lakshminarasimha, U.V. Varadaraju, J. Solid State Chem. 181 (2008) 2418.
[9] Z. Yang, J. Tian, S. Wang, G. Yang, X. Li, P. Li, Mater. Lett. 62 (2008) 1369.
[10] X. Liu, C. Lin, J. Lin, Appl. Phys. Lett. 90 (2007) 081904.
[11] G. Blasse, G.P.M. van den Heuvel, T. Van Dijk, Chem. Phys. Lett. 62 (1979) 600.
[12] Y. Kondo, K. Tanaka, R. Ota, T. Fujii, Y.I. Ishikawa, Opt. Mater. 27 (2005) 1438.
[13] X. Zhang, J. Zhang, L. Liang, Q. Su, Mater. Res. Bull. 40 (2005) 281.
[14] J.Th.W. de Hair, J. Lumin. 18 (1979) 797.
[15] B. Chu, C. Guo, Q. Su, Mater. Chem. Phys. 84 (2004) 279.
[16] Y. Yu, Y. Liu, M. Song, J. Alloys Compd. 202 (1993) 47.
[17] M.K. Jung, W.J. Park, D.H. Yoon, Sens. Actuators B 126 (2007) 328.
[18] X.X. Wang, Y.L. Xian, G. Wang, J.X. Shi, Q. Su, M.L. Gong, Opt. Mater. 30 (2007) 521.
[19] M. Taibi, E. Antic-Fidancev, J. Aride, M. Lemaitre-Blaise, P. Porcher, J. Phys.: Condens. Matter 5 (1993) 5201.
[20] J.G. Pepin, J. Appl. Cryst. 14 (1981) 70.
[21] J. Tang, Z. Zou, M. Katagiri, T. Kako, J. Ye, Catal. Today 885 (2004) 93.